Existence of a Hexatic Phase in Porous Media

Ravi Radhakrishnan,[1] Keith E. Gubbins,[2] and Malgorzata Sliwinska-Bartkowiak[3]

[1]*Massachusetts Institute of Technology, 77 Massachusetts Avenue, 66-021, Cambridge, Massachusetts 02139*

[2]*North Carolina State University, 113 Riddick Labs, Raleigh, North Carolina 27695*

[3]*Institute of Physics, Adam Mickiewicz University, Umultowska 85, 61-614 Poznan, Poland*

(Received 7 August 2000; revised manuscript received 17 April 2002; published 25 July 2002)

Molecular simulations for simple fluids in narrow slit-shaped carbon pores exhibit crystal-hexatic and hexatic-liquid transitions that are consistent with Kosterlitz-Thouless-Halperin-Nelson-Young theory. The temperature range over which the hexatic phase is stable is dramatically widened under confinement. Remarkably, the transitions, which are continuous for a single adsorbed layer, become weakly first order when the pore can accommodate two molecular layers. Nonlinear dielectric effect measurements for CCl_4 and aniline in activated carbon fibers (pore width 1.4 nm) show divergence at these transitions, confirming the hexatic phase.

DOI: 10.1103/PhysRevLett.89.076101 PACS numbers: 68.35.Rh

Two-dimensional systems have a special significance for phase transitions in which continuous symmetry is broken (such as freezing transitions). The Mermin-Wagner theorem states that true long-range order cannot exist in such systems [1]. Nelson and Halperin [2] proposed the KTHNY (Kosterlitz-Thouless-Halperin-Nelson-Young) mechanism for melting of a crystal in two dimensions, which involves two transitions of the Kosterlitz-Thouless (KT) kind [3]: The crystal to hexatic transition occurs through the unbinding of dislocation pairs, and the hexatic to liquid transition involves the unbinding of disclination pairs. The KTHNY theory predicts that for the hexatic phase the correlation function associated with the bond orientational order parameter decays algebraically with exponent $0 < \eta_6 < 1/4$ (quasi-long-range orientational order), while there is only short-range translational order.

Early simulation studies on small, strictly two-dimensional systems failed to provide compelling evidence to support the KTHNY melting scenario (for a review, see Strandburg [4]). However, it was demonstrated by Bagchi *et al.* [5], using a systematic scaling analysis on large system sizes, and subsequently by Jaster [6], that the equilibrium properties of a two-dimensional system of disks with repulsive interactions are indeed consistent with the KTHNY theory of melting, suggesting the earlier studies were plagued by serious system size effects.

The hexatic phase was first observed experimentally in an electron diffraction experiment on a quasi-two-dimensional system of a thin film of a liquid-crystalline material (see [7] and references therein). However, the intrinsic presence of a herringbone symmetry and its coupling to the hexatic symmetry in multilayer liquid-crystalline films causes the phase behavior to be more complicated [8]. Quasi-two-dimensional systems consisting of micron-sized colloidal particles confined between parallel glass plates do not have this complication [9,10], but in some [9] cases are faced with the question of the attainment of thermal equilibrium because of large particle sizes compared to molecular dimensions.

Activated carbon fibers (ACF) possess microcrystallites made up of graphene sheets that tend to align in similar directions, with slit-shaped voids between the microcrystals. The spontaneous ordering of the molecules adsorbed in these voids into distinct two-dimensional molecular layers makes the adsorbed phase a quasi-two-dimensional system, with none of the complications mentioned above. Here, we investigate melting in a quasi-two-dimensional system consisting of simple, near-spherical molecules adsorbed in slit-shaped pores, using both molecular simulation and experiment. The results are compared with the predictions of KTHNY theory.

In the simulations, carbon tetrachloride is chosen as the adsorbate to make contact with recent experimental studies of this system. The fluid-wall potential was modeled to be of the form of the "10-4-3" Steele Potential, with parameters chosen to represent the strongly attractive graphite pore [11]. The fluid-fluid Lennard-Jones (LJ) parameters were chosen to reproduce the bulk freezing temperature at 1 atm pressure [12]. Two pore widths, $H = 1\sigma_{ff} + \sigma_{fw} = 0.911$ nm and $H = 2\sigma_{ff} + \sigma_{fw} = 1.41$ nm, where H represents the shortest distance between the planes passing through the carbon nuclei on the surface of the opposing pore walls, were chosen, so that the adsorbed phase had one and two molecular layers of CCl_4, respectively. The calculations for the larger pore width also enable a direct comparison with experimental measurements for CCl_4 confined in porous activated carbon fiber ACF A-10, of mean pore width $H = 1.4$ nm. The extent of the rectilinear simulation cell was $180\sigma_{ff} \times 180\sigma_{ff}$ (93 nm $\times$ 93 nm) in the xy plane so that correlations up to $90\sigma_{ff}$ were captured in the simulations (z is normal to the pore walls). Periodic boundary conditions were used in the x and the y dimensions. We expect the approximation of a structureless graphite wall to be a good one here, since the diameter

of the LJ molecule (0.514 nm) is much larger than the C-C bond length in graphite (0.14 nm). We use the Landau-Ginzburg formalism [12] to calculate the free energy surface as a function of the hexatic bond-orientational order parameter, $\overline{\Psi}_{6,j}$ in layer j, as defined in Ref. [12].

Grand canonical Monte Carlo simulations were used to study the freezing behavior of LJ CCl_4 in our model graphite pore. Our simulation cell contained up to 64 000 molecules. The state conditions were such that the confined phase was in equilibrium with bulk LJ CCl_4 at 1 atm pressure. The simulations were started from a well equilibrated confined liquid phase at $T = 400$ K, and in successive simulation runs the temperature was reduced. Equilibration was for a minimum of eleven billion steps. The two-dimensional, in-plane positional and orientational correlation functions [$g_j(r)$ and $G_{6,j}(r)$ of layer j], were monitored to keep track of the nature of the confined phase. The positional pair correlation function is the familiar radial distribution function. The bond orientational pair correlation function is $G_{6,j}(\rho) = \langle \Psi^*_{6,j}(0)\Psi_{6,j}(\rho)\rangle$, where $\vec{\rho} = x\hat{e}_x + y\hat{e}_y$.

Our results for the two confined molecular layers of CCl_4 at three different temperatures were as follows [13]: The high temperature phase at $T = 360$ K was characterized by an isotropic $g(r)$ and exponentially decaying $G_{6,j}(r)$, and, hence, was a liquid. At $T = 330$ K, the positional pair correlation function was isotropic and the orientational correlation function decayed algebraically, a signature of the hexatic phase. At $T = 290$ K, the confined phase was a two- dimensional hexagonal crystal, with quasi-long-range positional order and long-range orientational order [13]. These features were verified using system size scaling analysis as discussed below. Since simulation results are always for a finite system size, we have established the self-consistency of our calculations by computing the Ginzburg parameter [14], γ_{GL}, for the different phases as a function of temperature and system size:

$$\gamma_{\mathrm{GL}} = \frac{\langle \overline{\Psi}^2_{6,j}\rangle}{\langle \overline{\Psi}_{6,j}\rangle^2} = \frac{I(L)}{\langle \overline{\Psi}_{6,j}\rangle^2} - 1, \qquad (1)$$

where $L^2 \times H = V$, the volume of the system, and $I(L)$ is given by

$$I(L) = \frac{\int_V d\vec{\rho}\, G_{6,j}(\rho)}{\int_V d\vec{\rho}}. \qquad (2)$$

The Ginzburg parameter is calculated by numerically integrating Eq. (2). If $\gamma_{\mathrm{GL}} \ll 1$, the simulations are self-consistent, i.e., (i) fluctuations do not destroy the ordered phase observed in the simulations, and (ii) the scaling behavior is not mean-field-like. It is clear from Fig. 1 that, for system sizes greater than $60\sigma_{ff} \times 60\sigma_{ff} \times H$, and for the temperature range of our simulations, our results are self-consistent. Therefore, two system sizes, $60\sigma_{ff} \times 60\sigma_{ff} \times H$ and $180\sigma_{ff} \times 180\sigma_{ff} \times H$, were used for system size scaling analysis. In order to study the scaling properties of the orientational correlation function, we plot $\log[I(L_B)/I(L)]$ as a function of $\log[L_B/L]$ in Fig. 2, where L was chosen to be $180\sigma_{ff}$ and three different values, $L_B = 60\sigma_{ff}$, $90\sigma_{ff}$, and $135\sigma_{ff}$, were used. The integral $I(L_B)$ is evaluated from $G_{6,j}(\rho)$ for the $180\sigma_{ff}$ system, by integrating over a subvolume of dimension $L_B \times L_B \times H$ instead of the total volume. A slope of -2 corresponds to having a finite correlation length (liquid), a slope of $-1/4$ corresponds to an algebraic decay of the orientational correlation function with exponent $-1/4$ (hexatic), and a zero slope corresponds to true long-range order [5]. In Fig. 2, the lines correspond to the scaling predicted by the KTHNY theory [5] and the symbols are our simulation results at three different temperatures; agreement between the simulations and theory is excellent. Therefore, the correlations in the one-layer system and the two-layer system are both consistent with the KTHNY predictions.

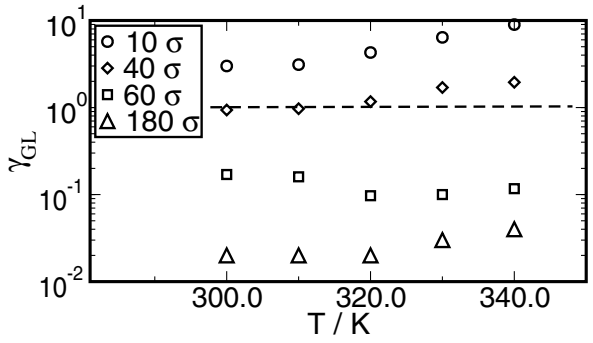

FIG. 1. Ginzburg parameter, γ_{GL}, for four different system sizes: $(10\sigma_{ff} \times 10\sigma_{ff} \times H)$, $(40\sigma_{ff} \times 40\sigma_{ff} \times H)$, $(60\sigma_{ff} \times 60\sigma_{ff} \times H)$, and $(180\sigma_{ff} \times 180\sigma_{ff} \times H)$. The simulations are for a pore width, $H = 1.4$ nm, consisting of two adsorbed layers of CCl_4. Finite system size calculations are self-consistent in the regime $\gamma_{\mathrm{GL}} \ll 1$.

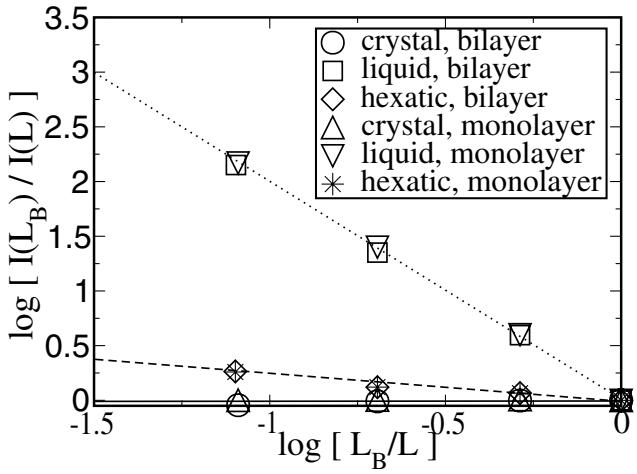

FIG. 2. System size scaling analysis for two systems with different pore widths, $H = 0.91$ nm and $H = 1.4$ nm. The error bars are of the same size as the symbols.

The Landau free energy surface, $\Lambda[\overline{\Psi}_{6,j}] = -k_B T \log P[\overline{\Psi}_{6,j}]$, where $P[\overline{\Psi}_{6,j}]$ is the probability distribution of the order parameter, was calculated using umbrella sampling [12] for the two pore widths at two different temperatures. Since our aim was to determine the order of the phase transition using the Lee-Kosterlitz scaling analysis [15] of the free energy surface, we obtained the Landau free energy functions at the exact transition temperatures for the corresponding system size. This was done as follows: The Landau free energy surface was calculated at a temperature close to the transition, from which we calculated the grand free energies at that temperature [12]. Then, by numerically integrating the Clausius-Clapeyron equation, $d(\Omega/T)/d(1/T) = \langle U \rangle - \mu \langle N \rangle$, we located the exact transition temperature. The Landau free energy function was recalculated at the transition temperature by using a weighting function equal to $\exp(\beta \Lambda[\overline{\Psi}_{6,j}])$ from the initial calculation. This procedure was repeated for each system size.

Shown in Fig. 3 are the Landau free energy plots for the smaller pore width $H = 0.91$ nm [curves (1) and (2)], for two different system sizes at their respective liquid-hexatic transition temperatures. The presence of the two phases ("L" and "H") of the system is clearly seen along with their relative thermodynamic stabilities; the nature of these phases was determined from the positional and orientational correlation functions. The free energy barrier between the liquid and the hexatic phases is seen to be $\approx 4k_B T$, and more importantly is system size independent. This is a clear indication of a second order phase transition in the thermodynamic limit [15], and is consistent with the predictions of the KTHNY theory. A similar result was obtained for the hexatic-crystal transition by repeating these calculations at the hexatic-crystal transition temperatures for the two system sizes [13]. Also shown in Fig. 3 are the Landau free energy plots for the larger pore width [curves (3) and (4)], which has two layers of CCl_4 adsorbed, for two different system sizes at their respective hexatic-crystalline transition temperatures. Remarkably, the free energy barrier between the hexatic and crystalline phases is seen to be linearly dependent on system size, a clear indication of a first-order phase transition in the thermodynamic limit [15], contrary to the perfect 2D case of the KTHNY scenario. A similar result was obtained for the liquid-hexatic transition by repeating these calculations at the liquid-hexatic transition temperatures for the two system sizes [13].

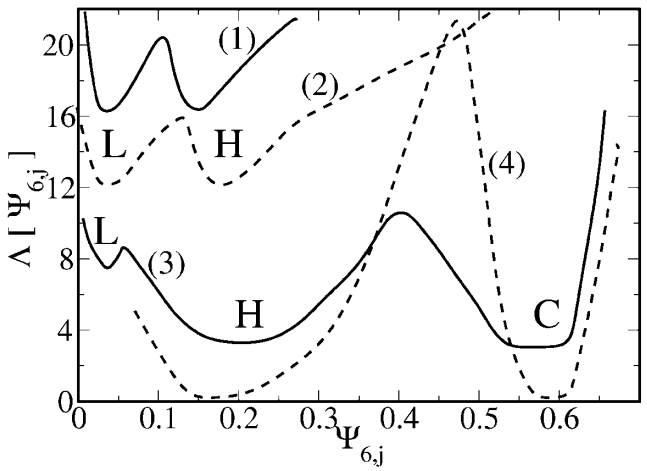

FIG. 3. Landau free energy functions for two different system sizes, $60\sigma_{ff}$ (solid lines) and $180\sigma_{ff}$ (dashed lines). Curves (1) and (2) are for pore width $H = 0.91$ nm at the liquid-hexatic transition, for the $60\sigma_{ff}$ system (curve 1, $T = 390$ K) and $180\sigma_{ff}$ (curve 2, $T = 387$ K) systems, respectively. Curves (3) and (4) are for pore width $H = 1.41$ nm at the hexatic-crystal transition, for the $60\sigma_{ff}$ system (curve 3, $T = 293$ K) and $180\sigma_{ff}$ (curve 4, $T = 290$ K) systems, respectively.

The scaling of the order-parameter correlation functions (Fig. 2) is consistent with the KTHNY behavior for both pore widths, implying that it is the vortex excitations that govern the equilibrium behavior in these quasi-two-dimensional systems and that the melting transition is defect mediated. Moreover, for the quasi-two-dimensional monolayers, the Kosterlitz-Thouless transitions are continuous, while, for quasi-two-dimensional bilayers, the Kosterlitz-Thouless transitions become first order. We ascribe this deviation from 2D behavior to the interactions between the defect configurations in different layers. If we consider two planes of xy models interacting with each other, a higher entropy scenario exists, where a vortex in one layer is aligned with a vortex of the opposite winding number in the other layer, with the cores displaced by distance A. Such a situation corresponds to a free energy [13]:

$$\Delta F = \Delta F^{(\mathrm{KT})} + JA \log(L) - 2k_B T \log(1 + 2\pi A) + (\pi - 1) J' L^2, \quad (3)$$

where J is the interaction of nearest neighbors of spins with the same alignment, L is the in-plane distance between vortex cores, $\Delta F^{(\mathrm{KT})} = (2\pi J - 2k_B T)\log(L)$ is the Kosterlitz-Thouless free energy [3], and J' is the nearest-neighbor interaction between layers and, in general, can be different from J. Treating L as the order parameter, the free energy profile is obtained by the locus of points that minimize ΔF, the variational parameter being A. The locus of points minimizing ΔF is qualitatively different from the true KT behavior, given by $\Delta F^{(\mathrm{KT})}$. In particular, at small separations of the vortices, the bound state actually exists as a metastable state for $T > T_c$, a clear signature of a first-order phase transition [13].

To seek experimental evidence for the confined hexatic phase, we have carried out differential scanning calorimetry (DSC) and nonlinear dielectric effect (NDE) measurements for CCl_4 and aniline confined in an activated carbon fiber (ACF-10) material having a mean pore size of

TABLE I. Transition temperatures from simulation and experiment for CCl_4 and aniline in ACF-10.

	Low T_c/K (H/C)		High T_c/K (L/H)	
Fluid	Simulation	Experiment	Simulation	Experiment
CCl_4	293	298,[a] 295[b,c]	348 K	353,[a,b] 352[c]
Aniline	296 [16]	298,[b] 299[c]	336 [16]	324,[b] 323[c]

[a]DSC. [b]DRS [16]. [c]NDE.

$H = 1.4$ nm. This material is known to have slit-shaped pores having a narrow pore size distribution [12,13]. In addition, dielectric relaxation spectroscopy (DRS) measurements have been carried out for aniline in this material [16]. The DSC scans show peaks, and the NDE and DRS measurements show sharp changes, indicating phase transitions at temperatures close to those predicted in the simulations, as shown in Table I. These results also show that the hexatic phase is stable over a wide temperature range, 55 K for CCl_4 and 26 K for aniline. The DRS measurements [16] for aniline provide the dielectric relaxation times; for the temperature regions below 298 K and above 324 K these times are typical of crystal and liquid phases, respectively, while between 298 and 324 K the times are of the order of 10^{-5} s, typical of a hexatic phase.

For both CCl_4 and aniline, we observed large values for the NDE $= \Delta\chi/E^2$ near the two transition temperatures. Here $\Delta\chi$ is the change in the dielectric susceptibility in a strong electric field E [17]. The NDE diverged at these transition points, and the divergence was consistent with the scaling behavior $1/\text{NDE} \sim \exp(-A/|T - T_c|^{\gamma})$, with $\gamma = 0.5$ for the liquid-hexatic (high temperature) transition and $\gamma = 0.37$ for the hexatic-crystal (low temperature) transition, in agreement with KTHNY theory [13]. NDE results for CCl_4 in ACF are shown in Fig. 4.

In conclusion, we reiterate our important findings: (i) Simulations and system size scaling confirm the existence of the hexatic phase in pores, even in the thermodynamic limit. Experimental results show strong support for the hexatic phase in ACF. (ii) The hexatic phase is stabilized in the pore relative to the bulk for strongly attracting walls, and becomes more stabilized as the strength of the fluid-wall interaction increases [12]. Thus, the T range over which the hexatic phase is observed is much larger in confined systems than in bulk ones. (iii) In confined systems, it is easy to observe the crystalline-hexatic and hexatic-liquid transitions even for *simple* fluids (e.g., inert gases, CCl_4)—there is no need for complex molecules (liquid crystal forming) or colloidal suspensions. (iv) We find second order transitions when the pore contains only one adsorbed layer. When the pore width is increased to allow two adsorbed layers, the behavior changes to a first-order transition. This change in behavior is explained by interaction between vortices in different adsorbed layers.

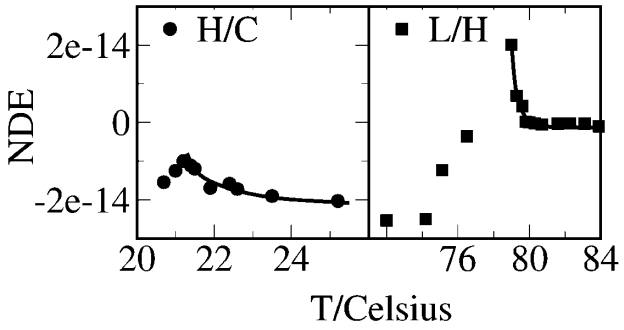

FIG. 4. NDE in m^2/V^2 vs T for CCl_4 confined in ACF at one atm, showing liquid-hexatic (L/H) and hexatic-crystalline (H/C) transitions. The symbols correspond to the experimental measurements and the solid lines are fits to the scaling laws with exponents from KTHNY theory.

This work was supported by grants from the National Science Foundation (Grant No. CTS-9908535) and the Maria Sklodowska-Curie Joint fund. Computing resources were provided by National Partnership for Advanced Computational Infrastructure (Grant No. MCA93S011).

[1] N. D. Mermin and H. Wagner, Phys. Rev. Lett. **17**, 1133 (1966).
[2] D. R. Nelson and B. I. Halperin, Phys. Rev. B **19**, 2457 (1979).
[3] J. M. Kosterlitz and D. J. Thouless, J. Phys. C **5**, L124 (1972).
[4] K. J. Strandburg, Rev. Mod. Phys. **60**, 161 (1988).
[5] K. Bagchi, H. C. Andersen, and W. Swope, Phys. Rev. Lett. **76**, 255 (1996).
[6] A. Jaster, Phys. Rev. E **59**, 2594 (1999).
[7] J. D. Brock, R. J. Birgeneau, J. D. Lister, and A. Aharony, Phys. Today **42**, No. 7,52 (1989); C. F. Chou, A. J. Jin, S. W. Huang, and J. T. Ho, Science **280**, 1424 (1998).
[8] D. L. Lin, J. T. Ou, L. P. Shi, X. R. Wang, and A. J. Jin, Europhys. Lett. **50**, 615 (2000).
[9] A. H. Marcus and S. A. Rice, Phys. Rev. E **55**, 637 (1997); C. A. Murray and D. H. Van Winkle, Phys. Rev. Lett. **58**, 1200 (1988).
[10] K. Zhan, R. Lenke, and G. Maret, Phys. Rev. Lett. **82**, 2721 (1999).
[11] W. A. Steele, Surf. Sci. **36**, 317 (1973).
[12] R. Radhakrishnan, K. E. Gubbins, and M. Sliwinska-Bartkowiak, J. Chem. Phys. **116**, 1147 (2002).
[13] R. Radhakrishnan, K. E. Gubbins, and M. Sliwinska-Bartkowiak (to be published).
[14] P. M. Chaikin and T. C. Lubensky, *Principles of Condensed Matter Physics* (Cambridge University Press, Cambridge, England, 1995).
[15] J. Lee and J. M. Kosterlitz, Phys. Rev. Lett. **65**, 137 (1990).
[16] M. Sliwinska-Bartkowiak, R. Radhakrishnan, and K. E. Gubbins, Mol. Sim. **27**, 323 (2001).
[17] A. Chelkowski, *Dielectric Physics* (Elsevier, Amsterdam, 1980).